Combining brine or CO2 geothermal preheating with low-temperature waste heat: A higher-efficiency hybrid geothermal power system

Author(s):
Garapati, Nagasree; Adams, Benjamin; Fleming, Mark R.; Kuehn, Thomas H.; Saar, Martin O.

Publication date:
2020-12

Permanent link:
https://doi.org/https://doi.org/10.3929/ethz-b-000446448

Originally published in:
Journal of CO2 Utilization 42, https://doi.org/10.1016/j.jcou.2020.101323

Journal of CO2 Utilization 42 (2020) 101323

Contents lists available at ScienceDirect

Journal of CO2 Utilization

journal homepage: www.elsevier.com/locate/jcou

Combining brine or CO_2 geothermal preheating with low-temperature waste heat: A higher-efficiency hybrid geothermal power system

Nagasree Garapati [a,*], Benjamin M. Adams [b,**], Mark R. Fleming [c], Thomas H. Kuehn [c], Martin O. Saar [b,d,**]

[a] Department of Chemical and Biomedical Engineering, West Virginia University, Morgantown, WV, USA
[b] Geothermal Energy and Geofluids Group, Department of Earth Sciences, ETH-Zürich, Zürich, Switzerland
[c] Department of Mechanical Engineering, University of Minnesota, Minneapolis, MN, USA
[d] Department of Earth and Environmental Sciences, University of Minnesota, Minneapolis, MN, USA

ARTICLE INFO

Keywords:
CO_2 geothermal
Hybrid geothermal
Auxiliary geothermal heating
Low-temperature geothermal systems
Carbon capture utilization and storage (CCUS)

ABSTRACT

Hybrid geothermal power plants operate by using geothermal fluid to preheat the working fluid of a higher-temperature power cycle for electricity generation. This has been shown to yield higher electricity generation than the combination of a stand-alone geothermal power plant and the higher-temperature power cycle. Here, we test both a direct CO_2 hybrid geothermal system and an indirect brine hybrid geothermal system. The direct CO_2 hybrid geothermal system is a CO_2 Plume Geothermal (CPG) system, which uses CO_2 as the subsurface working fluid, but with auxiliary heat addition to the geologically produced CO_2 at the surface. The indirect brine geothermal system uses the hot geologically produced brine to preheat the secondary working fluid (CO_2) within a secondary power cycle.

We find that the direct CPG-hybrid system and the indirect brine-hybrid system both can generate 20 % more electric power than the summed power of individual geothermal and auxiliary systems in some cases. Each hybrid system has an optimum turbine inlet temperature which maximizes the electric power generated, and is typically between 100 °C and 200 °C in the systems examined. The optimum turbine inlet temperature tends to occur where the geothermal heat contribution is between 50 % and 70 % of the total heat addition to the hybrid system. Lastly, the CO_2 direct system has lower wellhead temperatures than indirect brine and therefore can utilize lower temperature resources.

1. Introduction

The total amount of extractable geothermal energy in the United States is estimated to be 200,000 EJ (exajoules), which is approximately 2000 times the U.S. annual primary energy consumption in 2005 [1]. Currently most geothermal power plants installed in the U.S. are located in California or Nevada, where high geothermal temperature gradients and relatively shallow subsurface fracture networks exist [2]. Generally, geothermal systems are high-enthalpy, located in areas with high geologic temperature gradients due to volcanically or tectonically active settings [3] or due to advective heat redistribution by groundwater flow [4]. However, in order to expand geothermal technology over a wider geographic region, geothermal systems must utilize the abundant, lower-temperature geologic resources. Electricity can be generated from low-temperature (i.e. < 150 °C) geothermal resources with a binary cycle [5,6]. Unfortunately, due to their low thermal efficiency and high capital costs, standard binary cycle power plants are often marginally economically attractive for geothermal power generation [6]. However, the generation efficiency of low-temperature geothermal resources can be increased by specialized geothermal systems, such as CO_2-Plume Geothermal (CPG) and hybrid-geothermal systems. This correspondingly can increase the economic viability of geothermal electricity generation.

CO_2-Plume Geothermal (CPG) is a novel geothermal power system that can generate more power than brine using low-temperature geothermal resources [7]. A CPG system uses CO_2 as the geologic heat extraction fluid in naturally permeable sedimentary basin formations. This combines low-temperature geothermal with carbon capture and

* Corresponding author at: Deparment of Chemical and Biomedical Engineering, West Virginia University, Morgantown, WV, USA.
** Corresponding authors at: Geothermal Energy and Geofluids Group, Department of Earth Sciences, ETH-Zürich, Zürich, Switzerland.
E-mail addresses: nagasree.garapati@mail.wvu.edu (N. Garapati), badams@ethz.ch (B.M. Adams), saarm@ethz.ch (M.O. Saar).

https://doi.org/10.1016/j.jcou.2020.101323
Received 27 May 2020; Received in revised form 27 August 2020; Accepted 18 September 2020
Available online 10 October 2020

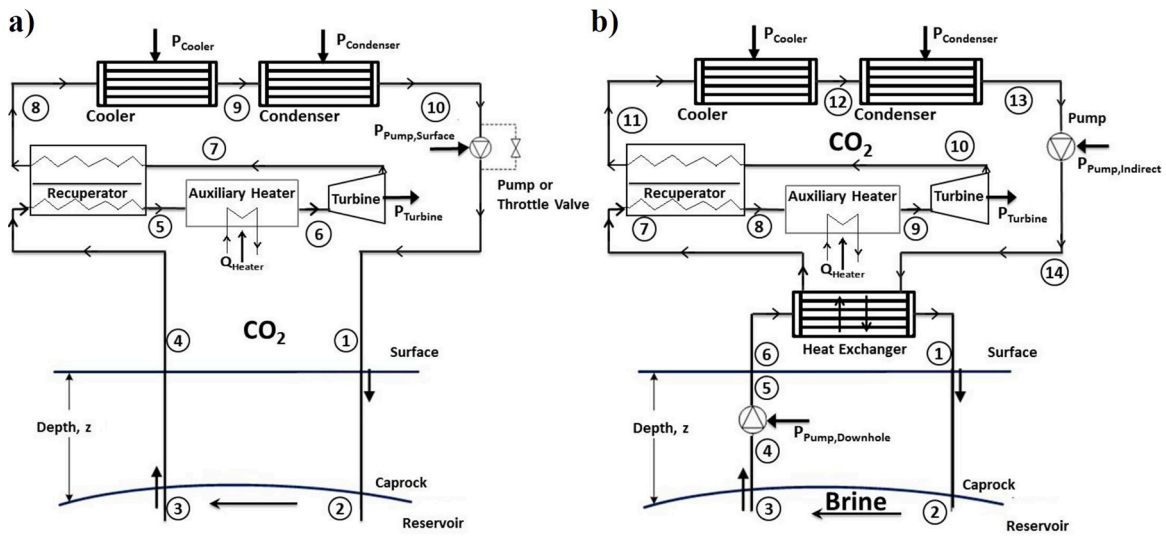

Fig. 1. Process flow diagrams for a) a direct CPG-hybrid system and b) an indirect brine-hybrid system (modified from [7]), where the latter uses CO_2 in the secondary loop. In either hybrid system, the auxiliary heater adds heat, from a here unspecified source, to the fluid immediately before the fluid is expanded in the turbine. The state point numbers are defined in the main text.

(geologic) storage (CCS), constituting a carbon capture, utilization, and storage (CCUS) system. This use of larger-scale, naturally permeable sedimentary reservoirs differentiates CPG from CO_2 Enhanced Geothermal Systems (CO_2-EGS), which use small, hydraulically stimulated fracture networks [8–13].

The use of CO_2 as the geologic working fluid has several advantages over brine: (1) CO_2 has a lower kinematic viscosity than brine, which reduces the frictional pressure losses in the geologic formation [8], (2) CO_2 has a lower mineral solubility than brine, reducing mineral scaling, which can reduce maintenance costs, and (3) CO_2 has a larger density variation with temperature than brine, which creates a thermosiphon in the vertical wells, that reduces (or eliminates) the need for circulation pumps [7,14–16]. Prior work has established the potential of CPG systems, demonstrating how they can generate more electric power than traditional brine systems at relatively low reservoir temperatures [7]. CPG systems can provide both baseload and dispatchable power [17], they employ CO_2 as an effective subsurface heat extraction fluid [18–21], and they can be augmented to store grid-scale energy as a so-called CO_2-Plume Geothermal Energy Storage (CPGES) system [22–24]. Lastly, they can be easily up-scaled to provide power generation comparable to fossil generators and to minimize capital cost [25].

A hybrid geothermal power plant uses geologically-produced fluid to preheat the working fluid in a secondary power cycle before it is heated by an auxiliary, higher temperature source. In principle, this hybrid approach can be beneficial, as the hybrid cycle converts the low-temperature geothermal heat to electricity at the thermal efficiency of the high-temperature energy source. Thus, the cycle generates more electricity than what the two facilities would generate separately. Additionally, the cost of electricity generation of a hybrid plant can typically be less than two individual, smaller plants, due to the economy of scale effect [26]. Lastly, auxiliary heating with relatively low-temperature geothermal working fluids can enable the use of currently available medium- to high-temperature energy conversion technologies (e.g. organic- or steam-based Rankine cycles, which are well established technologies for electricity generation), reducing the time and cost required to develop new technologies [27].

The auxiliary heat source for hybrid geothermal systems can be sourced from fossil fuels or renewable energy resources, such as solar-thermal or biomass energy. Waste heat is one such resource, with an estimated 161 GW_{th} avhailable in the United States alone [28]. However, in this manuscript, we explicitly avoid describing specific technologies or resources which are coupled with geothermal to make the hybrid plant. We do this to make the analysis and results as generalizable as possible and independent of the requirements of any technology.

Hybrid water-geothermal power plants have been previously studied. It was found that the power generated of a hybrid-geothermal plant can be higher than the sum of power generated by individual plants at a wide range of operating conditions [29–33] and can offer economic benefits due to capital cost reduction and cost reduction in operation and maintenance of the plant [34–37]. Bidini et al. [38] showed that when a geothermal plant and methane gas turbine are combined, the total power output can increase by 100 % and the fossil fuel thermal efficiency can increase above 40 % from their base case. Bruhn et al. [39] found that the geothermal preheating can be both economically and ecologically successful even without any subsidy, if the geothermal resource is found at close to steam power plants at moderate depths. Qin [40,41] developed a simulation tool to perform a technoeconomic analysis of geothermal aided power generation (GAPG) and results proved that the GAPG technology has higher thermodynamic first law efficiency and due to utilization of the existing infrastructure GAPG technology has economic advantages. Nsanzubuhoro et al. [42,43] investigated the optimum working conditions of a feedwater heater and geothermal preheater in a hybrid power plant to improve the power output. Based on their analysis, the replacement of the low-pressure feedwater heater with a geothermal preheater increased the power output and second law efficiency. More recently, the integration of low-temperature geothermal systems with solar energy resulted in higher second-law efficiency while reducing the cost of electricity production [26,44–48]. Zhou et al. [49,50] conducted technoeconomic feasibility analyses on hybrid solar–geothermal and hybrid geothermal–fossil fuel energy systems using Australian case studies. They found that the hybrid solar–geothermal power plant was affected by resource quality and weather conditions and the cost of electricity is about 23 % less than that of the stand-alone enhanced geothermal system (EGS). Their analyses also showed that a hybrid geothermal-fossil fuel system is economically feasible when hot dry rock (HDR) geothermal resources are located within 20 km from the power plants. The also developed reference maps to predict conditions when hybrid plant outperforms the stand-alone individual plants. However, all of these hybrid systems use water or brine as the subsurface heat exchange fluid.

Subsurface CO_2 can replace brine as the geologic working fluid in hybrid geothermal systems [51]. This may be advantageous because: 1) as geologic CO_2 is often a better reservoir heat extraction fluid than

Table 1
Study Parameters.

Parameter	Value
Reservoir Depth	2.5 km, 3.5 km, 4.5 km
Turbine Inlet Temperatures	100 °C to 600 °C in 50 °C increments
Reservoir Temperature Gradient	35 °C/km
Reservoir Permeability	50 mD
Well Diameter	0.41 m
Reservoir Well Spacing	707 m
Reservoir Production Time	15 years
Geologic Working Fluid	CO_2 -or- 20 wt% NaCl brine
Indirect Working Fluid	CO_2

water [8,20] and may thus also be a better subsurface working fluid for hybrid geothermal power plants, and 2) CPG systems require geologically sequestered CO_2 to operate, which may be supplied by a nearby fossil-fueled power plant with CO_2 capture. This nearby fossil-fueled plant may also provide a higher-temperature heat source for auxiliary heating of the geothermally pre-heated fluid.

Recently, Qiao et al. [52] conducted a technoeconomic analysis on a CPG supercritical CO_2 Brayton (CPG-sCO2) cycle using solar energy as auxiliary heat source. While this is CPG in that a CO_2-filled, 2.5 km deep sedimentary reservoir is used, they provide analysis which is inconsistent with CPG application. For instance, Qiao et al. [52] assumes a geothermal temperature gradient of 82 °C/km in the reservoir, providing a high-temperature heat source which is ideal for geothermal electricity generation; however, this value is much higher than 35 °C/km, which is common for non-faulted reservoirs found throughout much of the world and assumed in this paper. Ultimately, Qiao et al. [52] does not compare their system to any others (i.e. a control), which makes it difficult to generate conclusions. Thus, we compare auxiliary heating in this manuscript at common geothermal temperatures between CO_2 and water systems, both with and without hybridization.

In this paper, we find the electric power generation and thermal efficiency of direct CPG-hybrid systems and more-conventional indirect brine-based hybrid systems and compare them to separate geothermal-only and auxiliary-only systems. The comparison of hybrid geothermal system electric power generation to the sum of the electric power generations of separate geothermal-only and auxiliary-only systems shows the practicality of hybrid geothermal systems. This work is novel because the existing literature does not show the electric power generation of direct CO_2-based geothermal systems when auxiliary heating is applied. Additionally, brine-based hybrid systems tend to be coupled with high-temperature auxiliary heat sources, such as solar.

2. Geothermal power systems

In this work, we consider two hybrid geothermal electric power systems, also shown in Fig. 1:

1) *Direct CPG-hybrid system (*Fig. 1a*):* The geothermally heated and produced CO_2 is additionally heated with an auxiliary heat source before the CO_2 is directly expanded in a surface-plant turbine to generate electric power;
2) *Indirect brine-hybrid system (*Fig. 1b*):* The heat from the subsurface geothermal working fluid (brine) is transferred to a secondary working fluid (CO_2) in a surface-plant heat exchanger, after which the secondary working fluid is used to generate electric power.

We select direct CPG-hybrid systems for analysis as a direct CPG system yields higher electric power generation rates than indirect CO_2-based geothermal configurations [7]. Additionally, an indirect brine-based geothermal system is the current state-of-the-art for low- and medium-enthalpy geothermal systems.

Both the direct CPG and the indirect brine systems are similar to those investigated in our previous studies [7,19] with the important distinction that the hybrid systems add: 1) an auxiliary heater immediately upstream of the turbine inlet, and 2) a recuperator, to both the CPG- and the brine-based systems. The recuperator serves to preheat the fluid prior to entering the auxiliary heater using available heat at the turbine outlet, which improves efficiency. A primary variable of this work is the 'turbine inlet temperature' which is the fluid temperature leaving the auxiliary heater and entering the turbine (State 6 in Fig. 1a and State 9 in Fig. 1b). We consider these hybrid systems for the geologic reservoir conditions, well diameter, turbine inlet temperature, and working fluids shown in Table 1. The power plant parameters, along with equipment efficiencies, are detailed in Table 2. Nomenclature is provided in Table 4.

Table 2
Model and physical parameters of the geothermal reservoir.

Model Parameters	
Reservoir Configuration	Radially symmetric about the injection well
Number of Grid Cells, Vertical	34 non-uniform layers with fine grid at the reservoir top
Number of Grid Cells, Horizontal	50 logarithmically spaced layers with fine grid around injection and production wells
Well Orientation	Vertical (injection), Horizontal circular (production)
Well Spacing	707 m
Lateral Boundary Condition	No heat or fluid flow
Vertical Boundary Condition	No fluid flow; heat conduction using TOUGH2 semi-analytic model
Reservoir Working Fluid	CO_2 and/or 20 wt% H_2O-NaCl (brine)
Reservoir Thickness	300 m
Reservoir Horizontal Extent Radius	100 km
Reservoir Depth to Top	2500 m, 3500 m, 4500 m
Reservoir Production Temperature	102.5 °C, 137.5 °C, 172.5 °C
Reservoir Porosity	0.10
Reservoir Permeability, Horizontal	50×10^{-15} m^2 (50 mD)
Reservoir Permeability, Vertical	25×10^{-15} m^2 (25 mD)
Reservoir Thermal Conductivity	2.10 W/m/°C
Reservoir Rock Density	2650 kg/m^3
Reservoir Rock Specific Heat	1000 J/kg/°C
Geologic Temperature Gradient	35 °C/km
Relative Permeability & Capillary Pressure	van Genuchten [71] function
Residual Brine Saturation	0.30
van Genuchten, m	0.457
Residual CO_2 Saturation	0.05
van Genuchten, a	5.1×10^{-5} Pa^{-1}

It should be noted that both the direct CPG-hybrid and the indirect brine hybrid systems utilize CO_2, but in different ways. The direct CPG hybrid system (Fig. 1a) uses CO_2 in the subsurface reservoir and in the turbine. The indirect brine hybrid geothermal system (Fig. 1b) uses NaCl brine (i.e. saline aquifer) in the subsurface and CO_2 in the indirect Rankine cycle (the secondary loop) at the surface. Thus, both systems use CO_2 turbines, but employ fundamentally different reservoir fluids.

2.1. Direct CPG-Hybrid system

The direct CPG-hybrid system considered is a modified CPG system [7,20], with radial symmetry in the reservoir [19]. The CO_2 flow path through the reservoir, the wells, and the surface power plant is illustrated in Fig. 1a.

Cold CO_2 is injected at the surface at State 1, where it flows down the injection well to State 2, gravitationally compressing adiabatically to a supercritical fluid within the injection well. The CO_2 wellbore model is

described in Adams et al. [7]. The supercritical CO_2 flows through the reservoir and is heated to a temperature determined by the TOUGH2 model, reaching the bottom of the production well at State 3. The CO_2 then rises adiabatically [53] through the production well to the surface at State 4. At the surface, the CO_2 is first heated isobarically in a recuperator to State 5 and is then further heated isobarically by the auxiliary heater to a specified turbine inlet temperature from Table 1 (State 6). The heated fluid is expanded through a turbine for power generation to State 7, where the backpressure is set to 10 kPa above the saturation pressure of CO_2 at 22 °C. The turbine outlet temperature can be greater than the geothermal wellhead temperature (State 4), thus heat from the fluid leaving the turbine is first extracted using a recuperator between States 7 and 8, which is used to preheat the fluid between States 4 and 5. The recuperator has a specified effectiveness of 0.90.

The fluid is then cooled before being condensed isobarically at 22 °C (i.e. the sum of the approach temperature of 7 °C and the ambient air temperature of 15 °C), which is selected based on Adams et al. [7]. The CO_2 cooling and condensing towers are closed-circuit, with no intermediate cooling water loops. The cooled CO_2 is then pumped or throttled from State 10 to State 1. The total amount of CO_2 produced at State 4 is reinjected at State 1 to maintain the reservoir CO_2 plume, thus, this system constitutes a closed loop, meaning that none of the originally sequestered CO_2 is released to the atmosphere and 100 % of the CO_2 is still geologically stored.

2.2. Indirect brine-hybrid system

The indirect brine-hybrid system uses the same reservoir geometry as the direct CO_2-hybrid system described above. The indirect brine-hybrid system is shown in Fig. 1b. The indirect system differs fundamentally from the direct system because the geologic fluid does not directly pass through the turbine but instead exchanges heat with a second working fluid in a heat exchanger. Here CO_2 is used as the second working fluid, but this could also be an organic fluid, i.e. constitute an Organic Rankine Cycle (ORC), as discussed in [7].

The flow path of the primary geologic working fluid and the secondary working fluid is illustrated in Fig. 1b. Cold brine is injected from the surface (State 1) into the reservoir (State 2) via a vertical injection well. In the reservoir, the brine flows from the injection well to the horizontal, circumferential portion of the production well, extracting heat from the reservoir and increasing the brine temperature to the reservoir temperature. The heated brine travels isobarically within the horizontal portion of the production well to the beginning of the vertical production well (State 3). In the vertical production well, a down-hole pump at 500 m depth (States 4–5) provides a sufficient pressure increase to prevent the brine from flashing at the surface (State 6). Similar to Adams et al. [7], we limit this production well pump pressure increase to 10 MPa. At the surface, heat is extracted from the brine in a heat exchanger (States 6 to 1) and transferred to the secondary working fluid, CO_2 (States 14 to 7), cooling the brine. The cooled brine exits the heat exchanger and is reinjected into the reservoir.

In the indirect brine-hybrid system, the re-injection temperature (State 1), and thus the heat transfer to the secondary working fluid, is limited by the saturation temperature of dissolved amorphous silica. In the reservoir, the brine is saturated with dissolved quartz. When the brine is produced to the land surface and cooled below the saturation temperature, quartz precipitates from the solution as amorphous silica. Quartz precipitation can cause scaling within pipes and other equipment and is avoided by injecting the brine at a temperature above the saturation temperature of amorphous silica [54]. Thus, we limit the re-injection temperature (State 1) to a minimum of 9.5 °C, 45 °C, and 82 °C, which are the saturation temperature for 20 wt% NaCl brine produced from depths of 2.5 km, 3.5 km, and 4.5 km, respectively.

For the purposes of this study, we select CO_2 as the secondary working fluid. CO_2 was previously found to have higher thermal efficiency than the organic fluid R245fa in low-temperature geothermal cycles due to "pinch-point" constraints [7]. Using a supercritical working fluid eliminates such 'pinch-point' issues [55–57].

In the Rankine cycle (Fig. 1b), the geothermally heated CO_2 (State 7) is heated further in the recuperator to State 8. Then the CO_2 is heated in an auxiliary heater to the specified 'turbine inlet temperature' in Table 1 (State 9). The CO_2 is then expanded in a turbine, generating electricity. As the turbine outlet temperature (State 10) still has substantial heat, it is used to preheat the CO_2 before the auxiliary heater. The cooled CO_2 (State 11) is isobarically reduced in temperature to its saturation point (State 11) and condensed to a liquid at a pressure 10 kPa above the saturation pressure of CO_2 at 22 °C (State 13). The CO_2 is then pumped to the optimal high-side pressure (State 14) which produces the highest net power (supplemental information in Adams et al. [7]). The recuperator effectiveness is again 90 %, which determines the recuperator outlet fluid temperatures (States 8 and 11).

3. Conceptual and numerical model

We numerically simulate the two hybrid power plants by employing a coupled model including the subsurface reservoir, the wellbores, and the surface power plant. The subsurface geothermal fluid and heat transfer is simulated using TOUGH2 [58,59], with the equations of state (EOS) modules ECO2N [60] and ECO2H [61] for reservoir temperatures below and above $T = 100$ °C, respectively. The vertical wells and surface power plant performance are simulated using Engineering Equation Solver (EES) [62]. The CO_2 property data are from Span and Wagner [63] and the brine property data are from the relationships provided by Driesner [64] and the IAPS-84 Steam Tables [65]. We couple TOUGH2 and EES iteratively via Microsoft Visual Studio.

3.1. TOUGH2-EES coupled modelling approach

We use an iterative approach, varying the mass flow rate, to solve for the maximum net power generated by each hybrid system. The maximum net power is determined by first simulating the subsurface reservoir (TOUGH2) with an initial mass flow rate guess. The resulting reservoir production pressure, production temperature, and injection pressure are used as boundary conditions in the EES vertical well and surface power model, which determines the electric power generated. This process is then repeated using different mass flow rates until a maximum net power from the surface plant is obtained. Additionally, we validate convergence with Non-linear Equation System Solver (NESS) [66] and found that convergence is achieved as long as the simulator time step did not exceed one year.

3.2. Subsurface model (TOUGH2-ECO2N)

We simulate each reservoir as a three-dimensional (3D), axisymmetric (and thus computationally two-dimensional) numerical model, using the properties given in Table 2. The simulated reservoir has a thickness of 300 m, and the computational domain extends out to a radius of 100 km, consistent with previous simulations [19]. The reservoir is assumed to be a closed formation, bounded by an impermeable caprock above and impermeable bedrock below. The horizontal grid uses a logarithmically increasing spacing with refinements around the injection and production wells. The vertical grid spacing decreases with elevation, with the highest resolution immediately below the caprock. The vertical injection well is located at the centerline of the reservoir (i.e. a radius of zero) and extends vertically over the entire 300 m reservoir thickness. The horizontal, circular production well is located just below the caprock at a radius of 707 m, consistent with previous simulations [19]. The top and sides of the reservoir have no-mass flow and no-heat flow boundary conditions. The reservoir is conductively heated from below using a semi-analytic heat transfer solution [59], and also has a no-mass flow boundary condition. The initial reservoir temperature is set using a typical continental geothermal

temperature gradient of 35 °C/km [67,68], resulting in initial reservoir temperatures of 102.5 °C, 137.5 °C, and 172.5 °C for reservoir depths of 2.5 km, 3.5 km, and 4.5 km, respectively. TOUGH2 assumes local equilibrium between the reservoir fluid and rock within each element. Thus, the fluid production temperature from the TOUGH2 model is the combined rock/fluid temperature at the production element.

The pore space in the reservoir is initially filled with 20 wt% NaCl brine for all systems. For CO_2-based geothermal systems (i.e., CPG) the CO_2 plume must be developed, displacing the native brine between the injection and production wells, before CPG operations can commence. The CO_2 plume is initially developed over 2.5 years, as described in [19], by injecting 10 Mtonnes of CO_2 into the reservoir with no fluid production, though brine can be extracted during this phase to establish CO_2 flow pathways [69]. The CO_2 injection rate is linearly increased from 0 to 5 $MtCO_2$/year over the first year, and remains constant at 5 $MtCO_2$/year for the remaining 1.5 years. After this 2.5-year plume development phase, the CO_2 concentration at the production well is greater than the 94 % CO_2 value that was thought to be the minimum for CO_2 turbomachinery [70]. However, recent discussions with turbine manufacturers have revealed that a much lower range of CO_2 concentrations is possible, due to the relatively small density difference between supercritical CO_2 and liquid water within a CO_2 turbine. Additionally, high CO_2 concentrations in the production well allow us to use a pure CO_2 wellbore model, which reduces computation time. Lastly, we run the TOUGH2 simulation in 1-year timesteps for 15 years. Thus, the results presented here represent the 15th year of geothermal operation.

3.3. Well and surface power plant models

The produced fluid in the CPG system contains mostly CO_2, with only small amounts of water dissolved in the CO_2 [19,72]; therefore, the fluid in the wells is assumed to be pure CO_2. The injection and production wells and the surface plant are simulated identically to Adams et al. [7], with the addition of an auxiliary heater and recuperator.

The net electric power generated is the gross turbine power plus the (negative) parasitic electric powers, given in Eq.s 1 and 2 for the direct CPG ($P_{Net,CPG}$) and indirect Brine ($P_{Net,Indirect}$) systems. The difference between the two systems is the number of pumps: the direct CPG system only has a surface injection pump, while the indirect brine system has both a downhole geofluid production pump and an indirect cycle pump. All powers are calculated identically to Adams et al. [7].

$$P_{Net,CPG} = P_{Turbine} + P_{Pump,Surface} + P_{Cooler} + P_{Condenser} \quad (1)$$

$$P_{Net,Indirect} = P_{Turbine} + P_{Pump,Downhole} + P_{Pump,Indirect} + P_{Cooler} + P_{Condenser} \quad (2)$$

The amount of heat added by the auxiliary heat resource, $\dot{Q}_{Aux}$, to achieve the desired 'turbine inlet temperature' (State 6 in Fig. 1a; State 9 in Fig. 1b), is the product of the CO_2 mass flow rate, $\dot{m}$, and the difference between auxiliary heater exit, h_{outlet}, and inlet, h_{inlet}, enthalpies, given in Eq. 3.

$$\dot{Q}_{Aux} = \dot{m}\,(h_{outlet} - h_{inlet}) \quad (3)$$

The recuperator is an isobaric counter-flow heat exchanger with a specified effectiveness, ε, of 0.90. The effectiveness (Eq. 4) determines the fluid exit temperatures. The energy extracted from one fluid is equal to the energy added to the other so the heat exchanger is assumed to be externally adiabatic. The effectiveness is equal to the energy exchanged, divided by the theoretical maximum energy that can be exchanged that in this case occurs when the outlet temperature of one fluid equals the inlet temperature of the other.

$$\varepsilon = \frac{[\dot{m}(h_{inlet} - h_{outlet})]_{actual}}{[\dot{m}(h_{inlet} - h_{outlet})]_{theory\ max}} \quad (4)$$

A recuperator is used only if the temperature of the CO_2 leaving the turbine is higher than the temperature of the CO_2 entering the high-pressure side of the recuperator. Thus, a recuperator is not used in all simulations.

To compare the hybrid power system results, reference power plants are necessary. A "geothermal-only" power plant has no auxiliary heating ($\dot{Q}_{Aux} = 0$), thus, the inlet and exit auxiliary heat exchanger temperatures are equal (T_5=T_6 in Fig. 1a and T_8=T_9 in Fig. 1b). The electric power generated for the geothermal-only plant, $P_{Net,Geo}$, is equivalent to the electricity generated in Eq.s 1 or 2, based on the geofluid type, where there is no auxiliary heating.

An "auxiliary-only" power plant is the indirect cycle of Fig. 1b with no geothermal heat input (T_7=T_{14}), but uses all auxiliary heat input to obtain the specified turbine inlet temperature. The secondary mass flowrate of the "auxiliary-only" system is set such that the total heat input of the "auxiliary-only" system is equivalent to the auxiliary heat input of a hybrid geothermal system with the same turbine inlet temperature. The electric power generated for the auxiliary-only system, $P_{Net,Aux}$, is equivalent to the electricity generated in Eq. 2, where both the geofluid flowrate and downhole production pump power are zero $(P_{Pump,Downhole} = 0)$.

3.4. Performance criteria

We calculate electric power output for direct CO_2-hybrid and indirect brine-hybrid configurations for depths of 2.5 km, 3.5 km, and 4.5 km, using nine turbine inlet temperatures, from 100 °C to 600 °C (Table 1). We also calculate the electric power output for geothermal-only (i.e. no auxiliary heating) and auxiliary-only (i.e. no geothermal heating) systems for the same configurations and depths. These results are also tabulated in the Appendix. Results are omitted where the turbine inlet temperature is less than the produced fluid temperature. The results are then compared using the following criteria.

3.4.1. Net secondary thermal efficiency

The net secondary thermal efficiency (NSTE) is the thermal efficiency of the auxiliary-only power plant on the surface (Eq. 5).

$$\eta_{th,Sec} = \frac{P_{Net,\ Aux}}{Q_{Aux}} \quad (5)$$

Here, $P_{Net,Aux}$ is the net electric power generated by the auxiliary-only system and Q_{Aux} is the auxiliary heat energy added to heat the fluid to attain the specified turbine inlet temperature.

3.4.2. Incremental net secondary thermal efficiency

It is useful to think of the increase in power of the hybrid system due to the auxiliary heat addition. This is represented by the incremental net secondary thermal efficiency (INSTE) from Buck et al. [74], given in Eq. 6.

$$\Delta\eta_{th,Sec} = \frac{P_{Net} - P_{Net,Geo}}{Q_{Aux}} \quad (6)$$

The INSTE is the difference between the hybrid system electric power, P_{Net}, and the geothermal-only electric power, $P_{Net,Geo}$, divided by the auxiliary heat input. The hybrid system electric power, P_{Net}, is equivalent to either Eq. 1 or 2, depending on the system type. This metric uses only the auxiliary heat source in the denominator as this tends to be the only metered heat source in the hybrid configuration (i.e. geothermal heat is generally considered to have no marginal cost). The INSTE is the effective thermal efficiency applied to the auxiliary heat source. Ideally, this should be greater than the thermal efficiency of the auxiliary-only system.

3.4.3. Hybrid power ratio

The hybrid power ratio is the net electric power generated by the hybrid geothermal plant, P_{Net}, divided by the sum of the powers of the

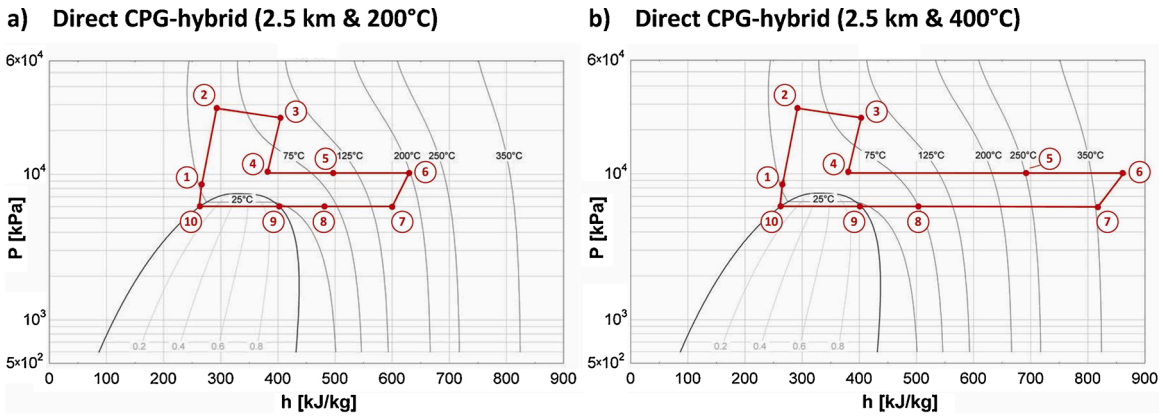

Fig. 2. Pressure-specific enthalpy (P-h) diagrams for the 2.5 km deep direct CPG-hybrid systems with turbine inlet temperatures of: a) 200 °C and b) 400 °C.

geothermal-only, $P_{Net,Geo}$, and auxiliary-only, $P_{Net,Aux}$, power plants (Eq. 7).

$$HPR = \frac{P_{Net}}{(P_{Net,Aux} + P_{Net,Geo})} \tag{7}$$

When this ratio is greater than one, the hybrid system generates more electric power than the sum of the individual systems and there is value in operating the hybrid system.

3.4.4. Geothermal heat fraction

The geothermal heat fraction is the ratio of heat added in the subsurface geothermal reservoir, $Q_{reservoir}$, to the combination of heat added in the subsurface and the auxiliary heat input (Eq. 8).

$$GHF = \frac{Q_{reservoir}}{(Q_{reservoir} + Q_{Aux})} \tag{8}$$

4. Results

First, we show cycle diagrams for the direct CPG-hybrid and indirect brine-hybrid systems. Then, we discuss the performance of the direct CPG-hybrid and the indirect brine-hybrid systems using the previously discussed metrics. Lastly, we find the fraction of geothermal heat to the total heat input into these systems.

4.1. Cycle state diagrams

The state points for a 2.5 km deep direct CO_2 system with a 200 °C turbine inlet temperature are shown in Fig. 2a, while the state points for a 2.5 km deep direct CO_2 system with a 400 °C turbine inlet temperature are shown in Fig. 2b.

The Rankine cycles are both trans-critical, i.e. the high-pressure (reservoir) side is supercritical while the low-pressure (surface) side is subcritical. Note that in the standard CPG cycle with no auxiliary heating, the turbine process line extends from State 4 down, intersecting line 9–10 at a vapor quality of approximately 60 %. Unlike steam turbines, a 60 % vapor quality is not problematic for CO_2 turbines as the vapor and liquid densities of CO_2 differ by only a factor of approximately four at that pressure. However, auxiliary heating will raise the cycle temperature and increase the thermal efficiency and power generation rates of a heat engine. Thus, CPG with auxiliary heating is thermodynamically preferred to regular CPG.

At a turbine inlet temperature of 200 °C (Fig. 2a), approximately 40 % of the heat addition at the surface is through the recuperator (States 4–5) of the total of the recuperator and auxiliary heat exchanger (States 4–6). Conversely, at a turbine inlet temperature of 400 °C, the recuperator heat addition increases to approximately 65 % of the total heat added at the surface. This is due to the relatively low temperature decrease (~50 °C) of the CO_2 between the turbine inlet and exit, when compared with steam. For comparison, steam turbines generally have saturated vapor at their exit (and thus high temperature decrease within the turbine). This small CO_2 temperature decrease through the turbine is a result of the relatively high CO_2 density within the turbine, compared with water vapor.

For an ideal gas undergoing an isentropic expansion, the pressure, P, and temperature, T, relationship, $P^{1-\gamma}T^{\gamma} = C$, is equal to a constant, C, where γ is the heat capacity ratio. The heat capacity ratio is the specific heat at constant pressure, c_p, divided by the specific heat at constant volume, c_v. When this pressure-temperature relationship is

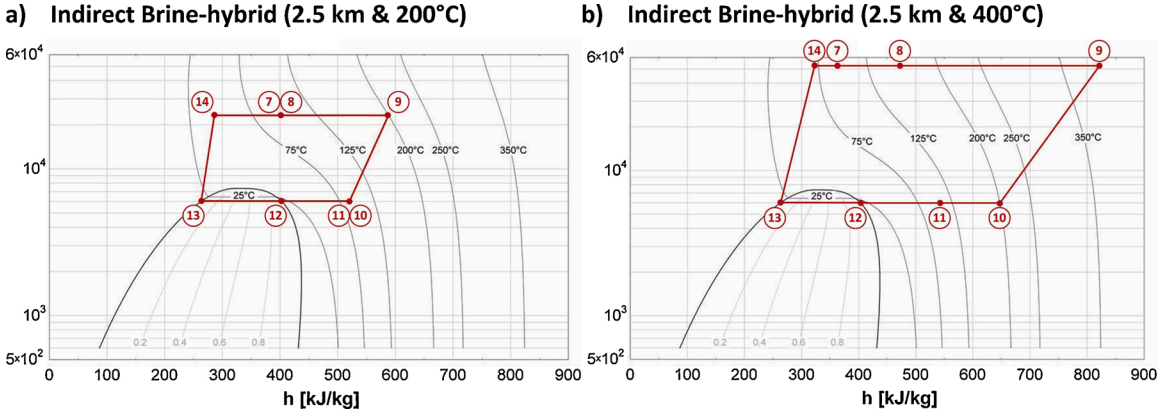

Fig. 3. Pressure-specific enthalpy (P-h) diagrams for the indirect brine-hybrid system with turbine inlet temperatures of: a) 200 °C and b) 400 °C. The indirect brine-hybrid system uses CO_2 as the secondary fluid in the Rankine cycle.

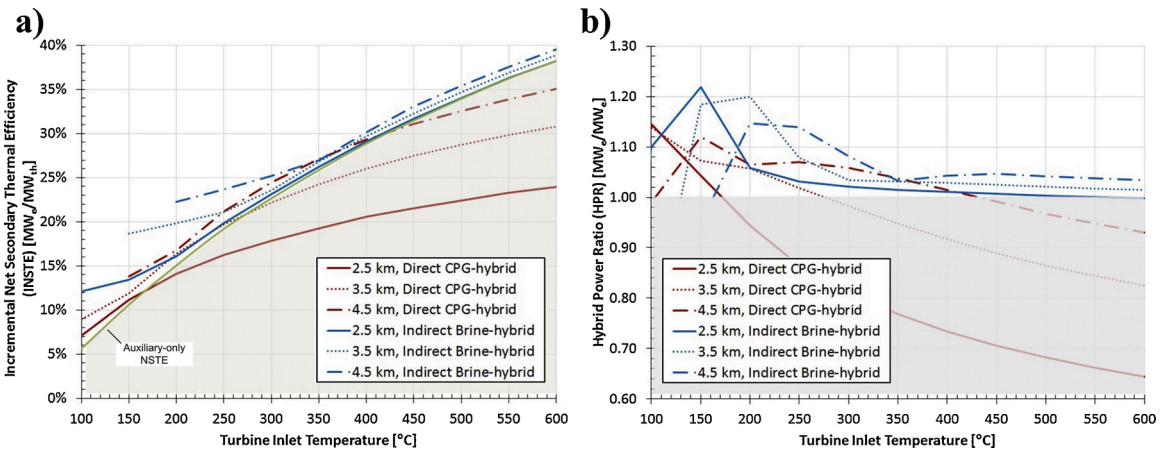

Fig. 4. a) Incremental net secondary thermal efficiency (INSTE) of direct CPG-hybrid (red lines), and indirect brine-hybrid (blue lines) power systems, compared with the net secondary thermal efficiency (NSTE) of an auxiliary-only power system (solid green line) at geothermal reservoir depths of 2.5 km, 3.5 km, and 4.5 km. b) The Hybrid power ratio (HPR) is the ratio of hybrid power generated to the sum of the geothermal-only and auxiliary-only systems. The HPR is shown for varying turbine inlet temperatures for geothermal reservoir depths of 2.5 km, 3.5 km, and 4.5 km.

differentiated and the ideal gas relation is substituted, the temperature sensitivity to pressure of an ideal gas, undergoing an isentropic expansion process, is $dT/dP = 1/(c_p \cdot \rho)$.

Despite being an ideal gas simplification, it can be seen that the decrease in fluid temperature, T, resulting from the pressure decrease through a turbine is strongly dependent on, and inversely related to, the fluid density, which differs greatly between CO_2 and water. For instance, at their respective turbine exit pressures (6 MPa for CO_2 and 0.1 MPa for water) and a temperature of 200 °C, the density of CO_2 is one to two orders of magnitude greater than water vapor (i.e. 70 kg/m^3 versus 1 kg/m^3). Conversely, at these same conditions, the specific heats of CO_2 and water vapor are roughly equivalent. Thus, CO_2 turbines tend to have high outlet temperatures, compared with water vapor turbines, and this heat should be recovered to maintain high cycle thermal efficiency.

Fig. 3 shows the pressure-enthalpy diagrams of the secondary Rankine cycles with turbine inlet temperatures of 200 °C (Fig. 3a) and 400 °C (Fig. 3b) for the 2.5 km deep indirect brine-hybrid systems. Similar to the direct CPG-hybrid cycles from Fig. 2, the turbine exit temperatures here are also substantially above the condensing temperature of 22 °C. However, unlike the direct CPG-hybrid cycles, the high-pressure side of the cycle is not constrained by the reservoir and may be optimized to generate the most power. This power optimization has already been accomplished and is available in the supplemental information of Adams et al. [7]. Thus, the high-side pressures for the 200 °C and 400 °C turbine inlet temperatures are approximately 22 MPa (Fig. 3a) and 51 MPa (Fig. 3b), respectively, compared with the fixed wellhead pressure of ~10 MPa in the direct CPG-hybrid cycle (Fig. 2).

Higher turbine inlet pressures lead to greater pressure drops through the turbine, which increase the power generated, despite the increase in inlet fluid density. Therefore, the higher turbine inlet pressures of the indirect brine cycles, as compared with the direct−CO_2 cycles with the same inlet temperatures, result in: lower turbine exit temperatures, more power generated, and less heat to be recuperated. Consequently, the 200 °C turbine inlet temperature case (Fig. 3a) does not need a recuperator and the 400 °C turbine inlet temperature case (Fig. 3b) has only ~25 % of its heat addition from recuperation (compared with 40 % and 65 % for the direct−CO_2 cycles).

4.2. Hybrid cycle comparison

The incremental net secondary thermal efficiency (INSTE) (Eq. 6) of the hybrid systems is compared to the net secondary thermal efficiency (NSTE) (Eq. 5) of the auxiliary-only power system in Fig. 4a. The INSTE is the increase in electric power generated per unit of auxiliary heat input of the hybrid system. When the INSTE of the hybrid system is greater than the NSTE of the auxiliary-only system (green line), the auxiliary heat addition in the hybrid system results in more electricity generated than the sum of the geothermal-alone and auxiliary-only systems.

The hybrid power ratio (HPR) (Eq. 7) in Fig. 4b shows the ratio of hybrid electric power generated to the sum of the individual geothermal-only and auxiliary-only systems. Thus, both plots in Fig. 4 are divided into two regions: 1) where the hybrid system is beneficial and generates more power than the sum of the individual geothermal and auxiliary-only plants (unshaded areas in Figs. 4a and 4b), and 2) where the hybrid system does not generate more power than the combined individual plants and should not be considered (shaded areas in Figs. 4a and 4b).

The hybrid systems tend to generate more power than the sum of the individual geothermal-only and auxiliary-only systems at low turbine inlet temperatures, as shown in Figs. 4a and 4b. For instance, at a turbine inlet temperature of 100 °C and a depth of 2.5 km, the direct CO_2-hybrid system generates 14 % more power (i.e. HPR = 1.14) than the summed power of the individual systems.

The direct CO_2 system has a lower wellhead temperature than the indirect brine system, allowing more heat of a given temperature to be transferred into the hybrid system and utilized. For both the direct CO_2 and indirect brine systems with a 2.5 km depth, the downhole fluid production temperature from the reservoir after 15 years is approximately 97 °C. The initial reservoir temperature at time-zero is 102.5 °C. However, the wellhead temperatures for each are very different: the CO_2 temperature reduces to 56 °C, while the brine temperature only reduces to 96 °C. The difference is due to the difference in expansion cooling of the fluids from decreasing pressure up the production well. The compressibility of the CO_2 results in higher wellhead pressure, but lower wellhead temperature than water. Conversely the water is nearly incompressible, thus the water temperature remains nearly constant and only the pressure decreases. Importantly, the wellbore temperature drop of the CO_2 is not an energy 'loss' (i.e. the CO_2 expansion is adiabatic). Thus, additional auxiliary heat can be readily transferred in the direct CO_2 system after it is produced from the wellhead from a 100 °C source whereas essentially none can be transferred in the indirect brine system. This is advantageous for the direct CPG-hybrid system, allowing it to better utilize a low-temperature heat resource.

The hybrid power ratio (HPR) is greater than one for the direct CO_2-hybrid systems with inlet temperatures less than 170 °C, 270 °C, and 430 °C for reservoir depths of 2.5 km, 3.5 km, and 4.5 km, respectively.

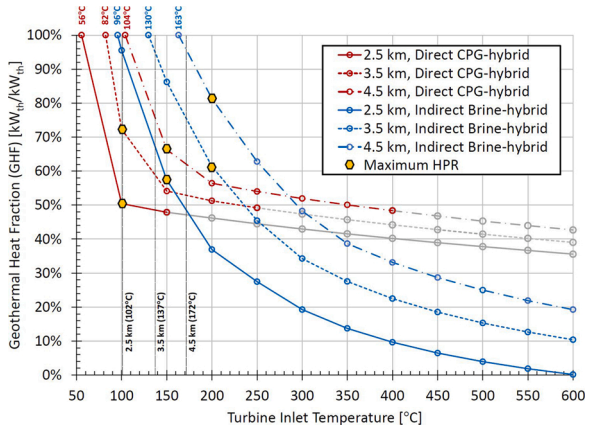

Fig. 5. Geothermal Heat Fraction (GHF) as a function of turbine inlet temperature for direct CPG-hybrid and indirect brine-hybrid systems. The temperature at 100 % GHF is the wellhead production temperature of the geofluid. The downhole reservoir production temperatures are given in black. Geothermal heat fractions with a hybrid power ratio less than one (HPR < 1), are shown in gray. Lastly, the turbine inlet temperature with the highest hybrid power ratio (HPR) for each system is marked with a yellow hexagon (see also Fig. 4b).

Conversely, the indirect brine-hybrid systems almost always have an HPR greater than one. Additionally, for a given turbine inlet temperature, the HPR of an indirect brine-hybrid system is almost always larger than a direct CPG-hybrid system. Thus, while both direct CPG and indirect brine systems yield applications where hybrid power ratios are greater than one, when a greenfield site is available, it may be advantageous to use an indirect brine system if auxiliary heating is preferred.

The direct CPG-hybrid systems do not always have a hybrid power ratio greater than one (i.e. the red lines within the shaded regions in Fig. 4). These cases tend to occur at high turbine inlet temperatures and low geologic temperatures, where significant auxiliary heat is required. In these pathological cases, the auxiliary heat addition in the direct CO_2 systems is at a suboptimal pressure. As previously discussed, the wellhead direct CPG system pressures are constrained by the reservoir and thus the high-side pressure is significantly lower than in the indirect system with the same turbine inlet temperature (i.e. turbine inlet pressure in Fig. 2b versus Fig. 3b). These cases should not be considered.

For all hybrid systems, there is an optimal turbine inlet temperature with the highest HPR. For each system, the HPR is one at the wellhead temperature. Also, the HPR decreases at high turbine inlet temperatures. Thus, each hybrid system provides the most value when operated at its optimal turbine inlet temperature, which tends to occur with lower-temperature auxiliary heat sources (i.e. lower turbine inlet temperatures). This is beneficial as waste heat is most common at lower temperatures and its availability decreases with increasing temperature. For instance, of the 161 GW_{th} waste heat potential in 2008 in the United States, 94 % has a temperature greater than 38 °C, 73 % has a temperature greater than 93 °C, and only 58 % has a temperature greater than 149 °C [28]. It should be cautioned that utilizing a high-temperature auxiliary heat source and merely using it to preheat geothermal fluid to a low temperature (e.g. using a 300 °C source to preheat fluid to a 100 °C turbine inlet temperature) is greatly inefficient and does not bring the same hybrid geothermal benefits as using a 100 °C resource to preheat a hybrid system to 100 °C.

4.3. Geothermal heat fraction

The geothermal heat fraction (GHF) is the fraction of heat utilized to generate electricity that is from the geothermal reservoir (Eq. 8). Fig. 5 shows the GHF for both the direct CO_2 and indirect brine systems as a function of turbine inlet temperature. At a GHF of 100 %, no auxiliary heat is added, and the system is "geothermal-only". The wellhead temperatures for these "geothermal-only" cases are provided along the top margin of Fig. 5. Additionally, the downhole reservoir production temperature is indicated for each of the three reservoir depths. The lines and data are shown in grey when the hybrid power ratio for a particular system is less than one (i.e. HPR < 1) and therefore to be avoided. Lastly, the temperature for each system with the highest HPR is indicated with a yellow hexagon.

Fig. 5 shows that the fraction of heat from the geothermal resource decreases as the turbine inlet temperature increases. For example, in the indirect brine-hybrid system with a 200 °C inlet temperature, approximately 36 % of the heat addition is from the geothermal resource. This value decreases to approximately 10 % when the turbine inlet temperature is 400 °C. In the indirect brine-hybrid system, this decrease in GHF is primarily due to two factors: the constant brine wellhead production temperature and the increased pump outlet CO_2 temperature within the secondary cycle. Conversely, in the direct CPG-hybrid system, the decrease in GHF is solely due to the constant CO_2 wellhead production temperature. We now explain each of these mechanisms.

The wellhead production temperature of the geologic fluid is constant across all turbine inlet temperatures for each system, thus increases in the turbine inlet temperature are only accomplished through increased auxiliary heating. For example, in the 2.5 km indirect brine-hybrid system, the wellhead temperature is fixed at 96 °C. This is the maximum temperature to which the geofluid can preheat the hybrid system. For example, if the turbine inlet temperature increases from 200 °C to 300 °C, the additional heat is provided by the auxiliary source, and thus the geothermal heat fraction necessarily decreases.

In the secondary (indirect) CO_2 cycle, higher turbine inlet temperatures yield higher pump outlet temperatures and, thus, lower geothermal heat addition. The high-side pressure of the secondary CO_2 cycle increases with increasing turbine inlet temperature to optimally generate power. As the CO_2 is pumped to increasing pressures, the resulting CO_2 pump outlet pressure also increases. As the geothermal preheater is located after the secondary pump, the geofluid can maximally increase the secondary fluid from the pump outlet temperature (State 14 in Fig. 1b) to the geofluid temperature (State 7 in Fig. 1b). Therefore, increasing the pump outlet temperature (due to the increase in turbine inlet temperature) will necessarily decrease the geothermal heat input into the system. This effect is most pronounced in the 2.5 km indirect brine-hybrid system with a 600 °C turbine inlet temperature, where the geothermal heat fraction is 0% because the pump outlet temperature is roughly equal to the wellhead brine temperature.

The direct CPG-hybrid systems show a plateau in geothermal heat fractions (GHF) at about 50 % above a turbine inlet temperature of 200 °C. This occurs despite having a fixed wellhead temperature and an increasing turbine inlet temperature. It also occurs in the region, where the hybrid power ratio (HPR) drops below one. This plateau is the result of recuperation and sub-optimal heat addition. As previously discussed, when CO_2 is expanded in a turbine, the exiting CO_2 is still very hot, which can be recuperated. Thus, we see in the direct CPG-hybrid systems that high turbine inlet temperatures are achieved with small additions of heat. Unfortunately, while the direct CPG-hybrid system is effective at recuperating heat, this does not lead to greater efficiencies. Instead, the direct CPG-hybrid system should only have auxiliary heating to a maximum temperature optimally determined by its pressure.

Lastly, Fig. 5 shows that the turbine inlet temperature with the highest hybrid power ratio tends to occur at a geothermal heat fraction of 50%–70%. This results in optimal turbine inlet temperatures between 100 °C and 200 °C. This high HPR region is an optimum between low temperatures, which do not get the benefit of auxiliary heating, and high temperatures, where geothermal preheating becomes insignificant.

Thus, we see from this geothermal heat fraction analysis that the hybrid system operates best at lower turbine inlet temperatures, where 50%–70% of the heat is derived from the geologic reservoir. As the CO_2 has lower wellhead temperatures than brine, the CO_2 has a lower

Table 3
Model parameters of the surface power plant.

Power Plant Constants	
Secondary (ORC) System Fluid	CO_2
Down-hole Production Well Pressure	Hydrostatic
Direct Turbine Isentropic Efficiency	78 %
ORC Turbine Isentropic Efficiency	80 %
Pump Isentropic Efficiency	90 %
Recuperator Effectiveness	90 %
Well Pipe Material	Bare CR13
Well Pipe Inner Diameter	0.33 m
Well Pipe Roughness	55 μm [73]
Condensing or Cooling Tower Approach Temperature	7 °C
Indirect Cycle Heat Exchanger Pinch-point Temperature	7 °C
Ambient Temperature	15 °C
Turbine Inlet Temperature	200 °C to 600 °C

Table 4
Nomenclature.

Abbreviations	
GHF	Geothermal Heat Fraction (MW_{th}/MW_{th})
HPR	Hybrid Power Ratio (MW_e/MW_e)
$INSTE$	Incremental Net Secondary Thermal Efficiency (MW_e/MW_{th})
$NSTE$	Net Secondary Thermal Efficiency (MW_e/MW_{th})
Variables	
c_p	Specific Heat at Constant Pressure ($kJ/kg/C$)
c_v	Specific Heat at Constant Volume ($kJ/kg/C$)
h_{outlet}	Auxiliary Heater Outlet Enthalpy (kJ/kg)
h_{inlet}	Auxiliary Heater Inlet Enthalpy (kJ/kg)
$\dot{m}$	Mass Flow Rate (kg/s)
P	Pressure (kPa)
$P_{Condenser}$	Condenser Power (MW_e)
P_{Cooler}	Cooler Power (MW_e)
$P_{Net,CPG}$	Net Electric Power Generated for a Direct CPG System (MW_e)
$P_{Net,Indirect}$	Net Electric Power Generated for an Indirect Brine System (MW_e)
P_{Net}	Net Electric Power Generated by the Hybrid System (MW_e)
$P_{Net,Aux}$	Net Electric Power Generated by the Auxiliary-only System (MW_e)
$P_{Net,Geo}$	Net Electric Power Generated by the Geothermal-only System (MW_e)
$P_{Pump,Downhole}$	Downhole Brine Production Pump Power (MW_e)
$P_{Pump,Surface}$	Surface CO_2 Injection Pump Power (MW_e)
$P_{Pump,ORC}$	Organic Rankine Cycle Pump Power (MW_e)
$P_{Turbine}$	Gross Power Generated by the Turbine (MW_e)
Q_{Aux}	Auxiliary Heat Rate (MW_{th})
$Q_{Reservoir}$	Geothermal Reservoir Heat Extraction Rate (MW_{th})
T	Temperature (C)
z	Reservoir Depth (m)
Greek symbols	
ε	Heat Exchanger Effectiveness (MW_{th}/MW_{th})
$\eta_{th,Sec}$	Net Secondary Thermal Efficiency (MW_e/MW_{th})
$\Delta\eta_{th,Sec}$	Incremental Net Secondary Thermal Efficiency (MW_e/MW_{th})
ρ	Fluid Density (kg/m^3)
γ	Heat Capacity Ratio, c_p/c_v (−)

optimal turbine inlet temperature and is therefore better suited to utilize low-temperature auxiliary resources. As the optimal auxiliary heating temperatures from this study were within the range of 100 °C–200 °C, these hybrid systems are also best coupled with waste heat sources as opposed to high-temperature (>500 °C) fossil sources. Thus, a direct CPG-hybrid system will use more of a given waste heat resource than an indirect brine-hybrid system.

5. Conclusions

Through simulations, we evaluated the electric power generation potential of two geothermal-hybrid systems: an indirect brine-hybrid system and a direct CPG-hybrid system. The indirect brine-hybrid system extracts heat from the geothermal reservoir with geologic brine while the direct CPG-hybrid system extracts heat using geologic CO_2. Both systems use auxiliary heating at the surface to increase the turbine inlet temperature. We compared each hybrid system to individual geothermal-only and auxiliary-only systems using the incremental net secondary thermal efficiency (INSTE), the hybrid power ratio (HPR), and the geothermal heat fraction (GHF). Our results allow us to make the following conclusions:

- *The direct CPG-hybrid system generates more electric power than the summed power of the individual geothermal-only and auxiliary-only systems below turbine inlet temperatures of 170 °C, 270 °C, and 430 °C for our 2.5 km, 3.5 km, and 4.5 km deep reservoirs, respectively.* These thresholds are established using our assumed common reservoir parameters, such as geothermal temperature gradient, permeability, etc. (Tables 1–3). For instance, at a reservoir depth of 2.5 km, the low-temperature heat addition to achieve a turbine inlet temperature of 100 °C increased the power generation by 14 % above the summed power of individual systems (i.e. hybrid power ratio of 1.14). At higher turbine inlet temperatures, the high-side cycle pressure is sub-optimal, as it is constrained by the wellhead pressure, and thus the power generation is low. At these high turbine inlet temperatures, where the HPR is less than one, the CPG-hybrid system should not be considered.
- *The indirect brine-hybrid system generates more electric power than the summed power of the individual geothermal-only and auxiliary-only systems in most cases, approaching a hybrid power ratio (HPR) of 1 as turbine inlet temperatures become large.* For instance, a 3.5 km indirect brine-hybrid system, with a turbine inlet temperature of 200 °C, generates 20 % more power than the summed power of the individual systems. At higher turbine inlet temperatures, the geothermal heat fraction decreases, reducing the HPR asymptotically towards one. Therefore, the geothermal-hybrid systems are best utilized at low turbine inlet temperatures, typically below 350 °C for geologic brine and 250 °C for geologic CO_2 (i.e. CPG) systems.
- *Both the direct CPG-hybrid and the indirect brine-hybrid systems have an optimal turbine inlet temperature, which provides the greatest hybrid power ratio (HPR). This tends to occur at a geothermal heat fraction (GHF) between 50 % and 70 %.* At low turbine inlet temperatures, the auxiliary heat is not utilized and thus the HPR is one. Conversely, at high turbine inlet temperatures, the geothermal heat input becomes insignificant and the hybrid value is diminished. For example, the highest HPRs occur at turbine inlet temperatures of 100 °C and 150 °C for the 2.5 km deep indirect brine-hybrid and the direct CPG-hybrid systems, respectively. Thus, these hybrid systems work best with low temperature waste heat streams. This is contrary to the 'traditional' concept of geothermal preheating, where a geothermal plant is coupled with high-temperature fossil fuel heat generation (i.e. > 500 °C).
- *The direct CPG-hybrid system has lower optimal turbine inlet temperatures than the indirect brine-hybrid system.* The direct CPG-hybrid system has lower wellhead temperatures than those for indirect brine-hybrid systems due to the expansion of the CO_2 up the production well. Thus, while the optimal turbine inlet temperatures for all hybrid systems tend to occur for geothermal heat fractions (GHF) of 50%–70%, the resultant corresponding turbine inlet temperatures for direct CPG-hybrid systems are lower. For instance, the wellhead temperatures of the 3.5 km systems are 82 °C for CO_2 and 130 °C for brine, resulting in optimal turbine inlet temperatures of 100 °C for direct CPG-hybrid and 150 °C for indirect brine-hybrid systems. Thus, the direct CPG-hybrid system can utilize lower temperature waste heat (i.e. auxiliary heat) than the indirect brine-hybrid system.

Data availability

The datasets used in this analysis are provided as supplemental information using Mendeley Data. Additionally, a subset of these data are given in tables in the Appendix.

CRediT authorship contribution statement

Nagasree Garapati: Conceptualization, Methodology, Software, Data curation, Formal analysis, Writing - original draft. **Benjamin M. Adams:** Conceptualization, Software, Formal analysis, Writing - original draft. **Mark R. Fleming:** Writing - original draft. **Thomas H. Kuehn:** Writing - review & editing, Supervision. **Martin O. Saar:** Writing - review & editing, Supervision, Funding acquisition.

Declaration of Competing Interest

The authors declare that they have no known competing financial interests or personal relationships that could have appeared to influence the work reported in this paper.

Acknowledgments

This work was supported in part by a Sustainable Energy Pathways (SEP) grant from the U.S. National Science Foundation (NSF) under Grant Number SEP-1230691, by the U.S. Department of Energy (DOE) under Grant Number DE-EE0002764, and by a grant from the Initiative for Renewable Energy and the Environment (IREE), a signature program of the Institute on the Environment (IonE) at the University of Minnesota (UMN), U.S.A. Martin Saar additionally thanks the Werner Siemens Foundation (Werner Siemens-Stiftung) for their endowment of the Geothermal Energy and Geofluids (GEG.ethz.ch) Group at ETH Zurich (ETHZ). We also thank the thoughtful comments from our two peer reviewers.

Any opinions, findings, conclusions, and/or recommendations expressed in this material are those of the authors and do not necessarily reflect the views of the NSF, DOE, IREE, IonE, UMN, ETHZ, or the Werner Siemens Foundation.

Appendix A

The tabulated simulation results are available in Table A1.

Table A1
The net power generated by direct CPG-hybrid and indirect brine power plants for varying reservoir depths and turbine inlet temperatures. The hybrid power, P_{Net}, auxiliary-only, $P_{Net,Aux}$, and geothermal-only, $P_{Net,Geo}$, powers are also given.

System	Depth (km) / Temperature (°C)	Turbine Inlet Temperature (°C)	P_{Net} (MW_e)	$P_{Net,Aux}$ (MW_e)	$P_{Net,Geo}$ (MW_e)	$P_{Net,Aux} + P_{Net,Geo}$ (MW_e)
Direct CPG Hybrid	2500 / 102.5	100	3.62	1.85	1.31	3.16
		150	5.53	3.99	1.31	5.31
		200	7.22	6.34	1.31	7.64
		250	8.73	8.78	1.31	10.09
		300	10.16	11.22	1.31	12.52
		350	11.54	13.71	1.31	15.02
		400	12.90	16.26	1.31	17.57
		450	14.24	18.86	1.31	20.17
		500	15.56	21.50	1.31	22.80
		550	16.87	24.17	1.31	25.47
		600	18.12	26.83	1.31	28.14
	3500 / 137.5	100	5.71	1.21	3.80	5.01
		150	9.60	5.15	3.80	8.95
		200	12.75	8.26	3.80	12.06
		250	15.62	11.54	3.80	15.34
		300	18.31	14.83	3.80	18.63
		350	20.88	18.21	3.80	22.01
		400	23.38	21.69	3.80	25.49
		450	25.83	25.24	3.80	29.04
		500	28.25	28.86	3.80	32.66
		550	30.64	32.52	3.80	36.32
		600	33.00	36.22	3.80	40.02
	4500/172.5	150	12.29	4.23	6.74	10.97
		200	17.04	9.26	6.74	16.01
		250	21.22	13.09	6.74	19.83
		300	25.08	16.96	6.74	23.70
		350	28.76	20.96	6.74	27.71
		400	32.30	25.10	6.74	31.84
		450	35.76	29.33	6.74	36.08
		500	39.05	33.63	6.74	40.37
		550	42.47	38.03	6.74	44.78
		600	45.79	42.48	6.74	49.23
Indirect Brine Hybrid	2500 / 102.5	100	1.06	0.085	0.88	0.97
		150	5.39	3.54	0.88	4.42
		200	12.50	10.93	0.88	11.82
		250	21.55	20.01	0.88	20.89
		300	34.31	32.72	0.88	33.60
		350	48.67	47.07	0.88	47.95
		400	64.47	62.93	0.88	63.81
		450	81.58	80.17	0.88	81.05
		500	99.83	98.62	0.88	99.50
		550	119.18	118.24	0.88	119.12
		600	139.41	138.79	0.88	139.67
	3500 / 137.5	150	6.74	1.39	4.30	5.69

(*continued on next page*)

Table A1 (*continued*)

System	Depth (km) / Temperature (°C)	Turbine Inlet Temperature (°C)	P_{Net} (MW_e)	$P_{Net,Aux}$ (MW_e)	$P_{Net,Geo}$ (MW_e)	$P_{Net,Aux} + P_{Net,Geo}$ (MW_e)
		200	14.37	7.68	4.30	11.98
		250	24.21	18.13	4.30	22.43
		300	37.99	32.43	4.30	36.73
		350	53.54	47.59	4.30	51.88
		400	70.61	64.36	4.30	68.65
		450	88.99	82.53	4.30	86.83
		500	108.46	101.90	4.30	106.20
		550	128.91	122.34	4.30	126.64
		600	150.19	143.69	4.30	147.99
		200	14.24	3.89	8.52	12.40
		250	24.17	12.70	8.52	21.22
		300	38.61	27.17	8.52	35.68
		350	56.07	45.79	8.52	54.30
	4500/ 172.5	400	76.47	64.79	8.52	73.30
		450	99.50	86.56	8.52	95.07
		500	120.60	107.20	8.52	115.72
		550	142.62	128.89	8.52	137.41
		600	165.44	151.50	8.52	160.02

References

[1] J.W. Tester, B. Anderson, A. Batchelor, D. Blackwell, R. DiPippo, E. Drake, J. Garnish, B. Livesay, M. Moore, K. Nichols, The future of geothermal energy: impact of enhanced geothermal systems (EGS) on the United States in the 21st century, Massachusetts Institute of Technology (2006).

[2] T. Reinhardt, New ways to produce geothermal power at lower temperatures, Power Engineering 117 (2013), 14-14.

[3] M.O. Saar, M.C. Castro, C.M. Hall, M. Manga, T. Rose, Quantifying magmatic, crustal, and atmospheric helium contributions to volcanic aquifers using all stable noble gases: implications for magmatism and groundwater flow, Geochem. Geophys. Geosystems (2005), https://doi.org/10.1029/2004GC000828.

[4] M.O. Saar, Review: geothermal heat as a tracer of large-scale groundwater flow and as a means to determine permeability fields, Hydrogeol. J. (2011), https://doi.org/10.1007/s10040-010-0657-2.

[5] M.H. Dickson, M. Fanelli, Geothermal Energy: Utilization and Technology, UNESCO, 2013. ISBN 978-1138991880.

[6] R. DiPippo, Geothermal Power Plants: Principles, Applications, Case Studies and Environmental Impact, Butterworth-Heinemann, 2012.

[7] B.M. Adams, T.H. Kuehn, J.M. Bielicki, J.B. Randolph, M.O. Saar, A comparison of electric power output of CO_2 Plume Geothermal (CPG) and brine geothermal systems for varying reservoir conditions, Appl. Energy 140 (2015) 365–377, https://doi.org/10.1016/j.apenergy.2014.11.043.

[8] D.W. Brown, A hot dry rock geothermal energy concept utilizing supercritical CO_2 instead of water, in: Proceedings of the Twenty-Fifth Workshop on Geothermal Reservoir Engineering, Stanford Univ., Stanford, CA,, 2000, pp. 233–238.

[9] K. Pruess, M. Azaroual, On the feasibility of using supercritical CO_2as heat transmission fluid in an engineered hot dry rock geothermal system. Proceedings of the Thirty-First Workshop on Geothermal Reservoir Engineering, Stanford University, Stanford, CA, 30 Jan.–1 Feb. 2006, 2006.

[10] K. Pruess, Enhanced Geothermal Systems (EGS) using CO_2 as working fluid – a novel approach for generating renewable energy with simultaneous sequestration of carbon, Geothermics 35 (4) (2006) 351–367.

[11] K. Pruess, On production behavior of enhanced geothermal systems with CO_2 as working fluid, Energy Convers. Manage. 49 (6) (2008), 1446-1454.

[12] T. Xu, K. Pruess, J. Apps, Numerical studies of fluid-rock interactions in enhanced geothermal systems (EGS) with CO_2 as working fluid, in: Proceedings of the Thirty-Third Workshop on Geothermal Reservoir Engineering Stanford University, Stanford, CA, January, 2008, pp. 28–30.

[13] K. Pruess, N. Spycher, Enhanced geothermal systems (EGS) with CO_2 as heat transmission fluid - a scheme for combining recovery of renewable energy with geologic storage of CO_2. Proceedings of the World Geothermal Congress 2010 Bali/ Indonesia, 25-29 April 2010, 2010.

[14] A.D. Atrens, H. Gurgenci, V. Rudolph, CO_2 thermosiphon for competitive geothermal power generation, Energy Fuels 23 (2009) 553–557.

[15] A.D. Atrens, H. Gurgenci, V. Rudolph, Electricity generation using a carbon dioxide thermosiphon, Geothermics 39 (2010) 161–169.

[16] B.M. Adams, T.H. Kuehn, J.M. Bielicki, J.B. Randolph, M.O. Saar, On the importance of the thermosiphon effect in CPG (CO_2 plume geothermal) power systems, Energy 69 (2014) 409–418, https://doi.org/10.1016/j.energy.2014.03.032.

[17] B.M. Adams, T.H. Kuehn, The complementary nature of CO_2-plume geothermal (CPG) energy production and electrical power demand, in: Proceedings of the ASME 2012 International Mechanical Engineering Congress & Exposition, IMECE2012-88704, November 9-15, 2012, Houston, Texas, USA, 2012, https://doi.org/10.1115/IMECE2012-88704.

[18] N. Garapati, J.B. Randolph, J.L. Valencia, M.O. Saar, CO_2-plume geothermal (CPG) heat extraction in multi-layered geologic reservoirs, Energy Procedia 63 (2014) 7631–7643, https://doi.org/10.1016/j.egypro.2014.11.797.

[19] N. Garapati, J.B. Randolph, M.O. Saar, Brine displacement by CO_2, energy extraction rates, and lifespan of a CO_2-limited CO_2-Plume Geothermal (CPG) system with a horizontal production well, Geothermics 55 (2015) 182–194, https://doi.org/10.1016/j.geothermics.2015.02.005.

[20] J.B. Randolph, M.O. Saar, Combining geothermal energy capture with geologic carbon dioxide sequestration, Geophys. Res. Lett. 38 (2011), L10401,, https://doi.org/10.1029/2011GL047265.

[21] J.B. Randolph, M.O. Saar, Coupling carbon dioxide sequestration with geothermal energy capture in naturally permeable, porous geologic formations: implications for CO_2 sequestration, Energy Procedia 4 (2011) 2206–2213.

[22] M.R. Fleming, B.M. Adams, J.B. Randolph, J.D. Ogland-Hand, T.H. Kuehn, T. A. Buscheck, J.M. Bielicki, M.O. Saar, High efficiency and large-scale subsurface energy storage with CO_2, in: Proceedings of the Forty-Third Workshop on Geothermal Reservoir Engineering, Stanford, CA,, 2018.

[23] Fleming, M.R., Adams, B.M., Kuehn, T.H., Bielicki, J.M., & Saar, M.O. (in preparation). The generation, storage, operation, and cost of a flexible CO_2-Plume Geothermal Energy Storage (CPGES) system in a low-temperature sedimentary reservoir.

[24] B.M. Adams, M.R. Fleming, J.M. Bielick, J. Hansper, S. Glos, M. Langer, M. Wechsung, M.O. Saar, Grid-scale energy storage using CO_2 in sedimentary basins: the cost of power flexibility, in: Proceedings of the European Geothermal Congress, Den Haag, The Netherlands, 11-14 June, 2019.

[25] Bielicki, J.M., Adams, B.M., Choi, H., Jamiyansuren, B., Taff, S.J., Saar, M.O., Buscheck, T.A., Ogland-Hand, J., in review. Cost-competitive geothermal electricity for geologic CO_2 storage. Energy Conversion and Management.

[26] C. Zhou, E. Doroodchi, B. Moghtaderi, An in-depth assessment of hybrid solar–geothermal power generation, Energy Convers. Manage. 74 (2013) 88–101.

[27] T. Kohl, R. Speck, A. Steinfeld, Using geothermal hybrid plants for electricity production from enhanced geothermal systems, Geothermal Resources Council Transactions 26 (2002) 315–318.

[28] A. Elson, R. Tidball, A. Hampson, Waste Heat to Power Market Assessment. Oak Ridge National Laboratory Publication ORNL/TM-2014/620, 2015, https://doi.org/10.2172/1185773.

[29] R. DiPippo, H. Khalifa, R. Correia, J. Kestin, Fossil superheating in geothermal steam power plants, Thirteenth Intersociety Energy Conversion Engineering Conference (1978) 1095–1101.

[30] J. Kestin, R. DiPippo, H. Khalifa, Hybrid geothermal-fossil power-plants, Mech. Eng. 100 (1978) 28–35.

[31] H.E. Khalifa, R. DiPippo, J. Kestin, Geothermal preheating in fossil-fired steam power plants, Thirteenth Intersociety Energy Conversion Engineering Conference (1978) 1068–1073.

[32] R. DiPippo, E.A. DiPippo, J. Kestin, H. Khalifa, Compound hybrid geothermal-fossil power plants: thermodynamic analyses and site-specific applications, J. Eng. Gas Turbine. Power 103 (1981) 797–804.

[33] R. DiPippo, Combined and hybrid geothermal power systems, in: R. DiPippo (Ed.), Chap. 14 in Geothermal Power Generation: Developments and Innovation, 1st. ed., Woodhead Publishing, Elsevier, Oxford, England, 2016, pp. 391–420.

[34] R. Parsons, System Design Verification of a Hybrid geothermal/coal Fired Power Plant. Report No. SAN-1572-T2, Burbank: City of Burbank and Ralph M. Parsons Company, 1978.

[35] R. Bettocchi, G. Cantore, G. Negri di Montenegro, E. Gadda, Thermodynamic and economic analysis on geothermal integrated combined-cycle power plants, in: Second Florence World Energy Research Symposium, Florence, Italy,, 1992, pp. 239–255.

[36] J. Buchta, A. Wawszczak, Economical and ecological aspects of renewable energy generation in coal fired power plant supported with geothermal heat, in: 2010 IEEE Electrical Power & Energy Conference, IEEE,, 2010, pp. 1–6.

[37] Q. Liu, L. Shang, Y. Duan, Performance analyses of a hybrid geothermal–fossil power generation system using low-enthalpy geothermal resources, Appl. Energy 162 (2016) 149–162.

[38] G. Bidini, U. Desideri, F.D. Maria, A. Baldacci, R. Papale, F. Sabatelli, Optimization of an integrated gas turbine–geothermal power plant, Energy Convers. Manage. 39 (1998) 1945–1956.

[39] M. Bruhn, Hybrid geothermal–fossil electricity generation from low enthalpy geothermal resources: geothermal feedwater preheating in conventional power plants, Energy 27 (2002) 329–346.

[40] J. Qin, A Technical and Economic Assessment of Geothermal Aided Power Generation, The School of Mechanical Engineering, The University of Adelaide, 2013.

[41] Y. Zhou, J. Qin, Optimisation of displacement selections and structures for the Geothermal aided Power Generation plant, Research Square (2020), https://doi.org/10.21203/rs.3.rs-27979/v1.

[42] C. Nsanzubuhoro, Optimisation of feedwater heaters and geothermal preheater in fossil-geothermal hybrid power plant, Engineering and the Built Environment (2019). University of Cape Town.

[43] C.N. Nsanzubuhoro, T. Bello-Ochende, A.G. Malan, Second law analysis of a fossil-geothermal hybrid power plant with thermodynamic optimization of geothermal preheater, Heat Transfer (2020) 1–22.

[44] Á. Lentz, R. Almanza, Solar–geothermal hybrid system, Appl. Therm. Eng. 26 (2006) 1537–1544.

[45] Ferguson, R., Shors, L., Bryden, K., Corns, S., 2010. Hybrid Power Solar Facilities. US Patent Application US20100154417A1.

[46] M. Astolfi, L. Xodo, M.C. Romano, E. Macchi, Technical and economical analysis of a solar–geothermal hybrid plant based on an Organic Rankine Cycle, Geothermics 40 (2011) 58–68.

[47] D. Tempesti, G. Manfrida, D. Fiaschi, Thermodynamic analysis of two micro CHP systems operating with geothermal and solar energy, Appl. Energy 97 (2012) 609–617.

[48] H. Ghasemi, E. Sheu, A. Tizzanini, M. Paci, A. Mitsos, Hybrid solar–geothermal power generation: optimal retrofitting, Appl. Energy 131 (2014) 158–170.

[49] C. Zhou, A fundamental study on hybrid geothermal energy systems, Univ. Newcastle Tyne Med. Gaz. (2014).

[50] C. Zhou, E. Doroodchi, B. Moghtaderi, Assessment of geothermal assisted coal-fired power generation using an Australian case study, Energy Convers. Manage. 82 (2014) 283–300.

[51] N. Garapati, J.B. Randolph, M.O. Saar, Superheating of low-temperature geothermal working fluids to boost electricity production: comparison between water and co₂ systems, in: Proceedings of the Fortieth Workshop on Geothermal Reservoir Engineering, Stanford University, Stanford, CA,, 2015.

[52] Z. Qiao, Y. Cao, P. Li, X. Wang, C.E. Romero, L. Pan, Thermoeconomic analysis of a CO_2 plume geothermal and supercritical CO_2 Brayton combined cycle using solar energy as auxiliary heat source, J. Clean. Prod. 256 (2020), 120374,, https://doi.org/10.1016/j.jclepro.2020.120374.

[53] J.B. Randolph, B. Adams, T.H. Kuehn, M.O. Saar, Wellbore heat transfer in CO_2-based geothermal systems, Geothermal Resources Council Transactions 36 (2012) 549–554.

[54] R. DiPippo, Simplified method for estimating the silica scaling potential in geothermal power plants, Geothermal Resources Council Bulletin (1985). May.

[55] Y.R. Li, J.N. Wang, M.T. Du, Influence of coupled pinch point temperature difference and evaporation temperature on performance of organic Rankine cycle, Energy 42 (2012) 503–509.

[56] Y.R. Li, J.N. Wang, M.T. Du, S.Y. Wu, C. Liu, J.L. Xu, Effect of pinch point temperature difference on cost-effective performance of organic Rankine cycle, Int. J. Energy Res. 37 (2013) 1952–1962.

[57] M. Ryms, T. Pyś, E. Klugmann-Radziemska, Adapting the pinch point analysis to improve the ORC design process, Int. J. Energy Res. 38 (2014) 29–40.

[58] K. Pruess, G. Moridis, C. Oldenburg, TOUGH2 User's Guide, Version 2.0, Lawrence Berkeley National Laboratory, Berkeley, California, 1999.

[59] K. Pruess, The TOUGH codes—a family of simulation tools for multiphase flow and transport processes in permeable media, Vadose Zone J. 3 (2004) 738–746.

[60] K. Pruess, ECO2N: A TOUGH2 Fluid Property Module for Mixtures of Water, NaCl, and CO_2, Lawrence Berkeley National Laboratory, Berkeley, California, 2005.

[61] N. Spycher, K. Pruess, A model for thermophysical properties of CO_2-brine mixtures at elevated temperatures and pressures, in: Proceedings of the Thirty-Sixth Workshop on Geothermal Reservoir Engineering, Stanford University, Stanford, CA, January, 2011.

[62] S. Klein, F. Alvarado, Engineering Equation Solver. F-Chart Software, Madison, WI, 2002.

[63] R. Span, W. Wagner, A new equation of state for Carbon Dioxide covering the fluid region from the triple point temperature to 1100 K at pressures up to 800 MPa, J. Phys. Chem. Ref. Data 25 (1996) 1509–1596.

[64] T. Driesner, The system H_2O–NaCl. Part II: correlations for molar volume, enthalpy, and isobaric heat capacity from 0 to 1000° C, 1 to 5000bar, and 0 to 1 X_{NaCl}, Geochim. Cosmochim. Acta 71 (2007) 4902–4919.

[65] L. Harr, J. Gallagher, G. Kell, NBS/NRC Steam Tables: Thermodynamic and Transport Properties and Computer Programs for Vapor and Liquid States of Water in SI Units, Hemisphere, New York, 1984.

[66] S.D.C. Walsh, N. Garapati, A.M.M. Leal, M.O. Saar, Calculating thermophysical fluid properties during geothermal energy production with NESS and Reaktoro, Geothermics 70 (2017) 146–154, https://doi.org/10.1016/j.geothermics.2017.06.008.

[67] H.N. Pollack, S.J. Hurter, J.R. Johnson, Heat flow from the Earth's interior: analysis of the global data set, Rev. Geophys. 31 (1993) 267–280.

[68] J.H. Davies, D.R. Davies, Earth's surface heat flux, Solid Earth 1 (2010) 5–24.

[69] M.R. Fleming, B.M. Adams, T.H. Kuehn, J.M. Bielicki, M.O. Saar, Benefits of using active reservoir management during CO_2-plume development for CO_2-plume geothermal (CPG) systems, in: Proceedings of the Forty-Forth Workshop on Geothermal Reservoir Engineering, Stanford University, Palo Alto, CA,, 2019.

[70] P. Welch, P. Boyle, New turbines to enable efficient geothermal power plants, Geothermal Resources Council Transactions 33 (2009) 765–772.

[71] M.T. Van Genuchten, A closed-form equation for predicting the hydraulic conductivity of unsaturated soils, Soil Sci. Soc. Am. J. 44 (1980) 892–898.

[72] M.R. Fleming, B.M. Adams, T.H. Kuehn, J.M. Bielicki, M.O. Saar, Increased power generation due to exothermic water exsolution in CO_2 Plume Geothermal (CPG) power plants, Geothermics 88 (2020), 101865.

[73] F.F. Farshad, H.H. Rieke, Surface roughness design values for modern pipes, Spe Drill. Complet. 21 (2006) 212–215.

[74] R. Buck, T. Brauning, T. Denk, M. Pfänder, P. Schwarzbözl, F. Tellez, Solar-hybrid gas turbine-based power tower systems (REFOS), J. Sol. Energy Eng. 124 (2002) 2–9.